The Journal of Immunology

Methamphetamine Causes Mitrochondrial Oxidative Damage in Human T Lymphocytes Leading to Functional Impairment

Raghava Potula, Brian J. Hawkins, Jonathan M. Cenna, Shongshan Fan, Holly Dykstra, Servio H. Ramirez, Brenda Morsey, Michael R. Brodie and Yuri Persidsky

J Immunol 2010; 185:2867-2876; Prepublished online 28 July 2010;
doi: 10.4049/jimmunol.0903691
http://www.jimmunol.org/content/185/5/2867

The Journal of Immunology is published twice each month by
The American Association of Immunologists, Inc.,
1451 Rockville Pike, Suite 650, Rockville, MD 20852

Print ISSN: 0022-1767 Online ISSN: 1550-6606.

Methamphetamine Causes Mitochondrial Oxidative Damage in Human T Lymphocytes Leading to Functional Impairment

Raghava Potula,* Brian J. Hawkins,† Jonathan M. Cenna,* Shongshan Fan,* Holly Dykstra,* Servio H. Ramirez,* Brenda Morsey,‡ Michael R. Brodie,‡ and Yuri Persidsky*

Methamphetamine (METH) abuse is known to be associated with an inordinate rate of infections. Although many studies have described the association of METH exposure and immunosuppression, so far the underlying mechanism still remains elusive. In this study, we present evidence that METH exposure resulted in mitochondrial oxidative damage and caused dysfunction of primary human T cells. METH treatment of T lymphocytes led to a rise in intracellular calcium levels that enhanced the generation of reactive oxygen species. TCR-CD28 linked calcium mobilization and subsequent uptake by mitochondria in METH-treated T cells correlated with an increase in mitochondrion-derived superoxide. Exposure to METH-induced mitochondrial dysfunction in the form of marked decrease in mitochondrial membrane potential, increased mitochondrial mass, enhanced protein nitrosylation and diminished protein levels of complexes I, III, and IV of the electron transport chain. These changes paralleled reduced IL-2 secretion and T cell proliferative responses after TCR-CD28 stimulation indicating impaired T cell function. Furthermore, antioxidants attenuated METH-induced mitochondrial damage by preserving the protein levels of mitochondrial complexes I, III, and IV. Altogether, our data indicate that METH can cause T cell dysfunction via induction of oxidative stress and mitochondrial injury as underlying mechanism of immune impairment secondary to METH abuse. ***The Journal of Immunology*****, 2010, 185: 2867–2876.**

Illicit drug abuse such as methamphetamine (METH) linked with risky sexual behavior and rapid progression of HIV-1 infection has radically changed the public health landscape at multiple levels. Recent studies have enumerated the deleterious effects of METH on various components of the immune system either by altering or suppressing the functions of distinct immune cell types (1–9). However, little is known about the direct effects of METH on T lymphocytes and how it may lead to compromises in regulation of immune homeostasis.

Mitochondria are critical for maintenance of the bioenergetic status of cells (10). Calcium, a secondary messenger of intracellular signaling, serves as the key link coupling cellular energy demand and mitochondrial energy production. In lymphocytes, mitochondrial calcium uptake is associated with an increase in mitochondrial bioenergetics (11) and formation of the immunological synapse (12). However, a consequence of mitochondrial calcium uptake is the production of reactive oxygen species (ROS) (13). Under physiological conditions, cellular redox balance is maintained by the equilibrium between formation and elimination of free radicals such as ROS and nitrogen species (RNS). Excessive generation of ROS/RNS or inadequate antioxidant defenses can cause damage of cellular structures and result in mitochondrial impairment (14). Oxidative stress inhibits complex enzymes in the electron transport chain that can severely disrupt mitochondrial respiration (15). Thus, being the predominant site of free radical production, mitochondria are common targets for the injury caused by oxidative species (10). Oxidative stress and mitochondrial damage have been implicated in numerous pathologic conditions, and oxidative stress is an underlying cause of METH-mediated neurotoxicity (16) and dysfunction of the brain endothelium (17).

The effects of oxidative stress on suppressed signal transduction, transcription factor activities, and decreased cytokine production in response to nonspecific and Ag-specific stimulation in T cells has been documented in several model systems (18). The ability of ROS to impair T lymphocyte function has been documented in diverse human pathologic conditions, including cancer, rheumatoid arthritis, AIDS, and leprosy (19–21). In this study, we evaluated the effects of METH exposure on primary human T cell ROS production and mitochondrial dysfunction. Pathophysiologically relevant concentrations of METH increased cytosolic calcium and enhanced ROS generation, which was blocked by a mitochondrial antioxidant. On addition of METH, changes in mitochondrial membrane potential, mitochondrial mass, and loss of complexes I, II, and III proteins of the electron transport chain (ETC) was observed in T cells. Furthermore, treatment of T cells with METH resulted in protein nitrosylation and impaired T cell function, including a decrease in cytokine secretion and proliferative responses.

*Department of Pathology and Laboratory Medicine and †Department of Biochemistry, Temple University School of Medicine, Philadelphia, PA 19140; and ‡Department of Pharmacology and Experimental Neuroscience, University of Nebraska Medical Center, Omaha, NE 68164

Received for publication November 16, 2009. Accepted for publication June 24, 2010.

This work was supported by National Institutes of Health Grants R21 DA0249791 (to R.P), DA025566, and R01AA017398 (to Y.P.) as well as developmental grants (to Y.P.). B.J.H. was supported by National Institutes of Health Grant K99HL094536.

Address correspondence and reprint requests to Dr. Raghava Potula, Department of Pathology and Laboratory Medicine, Temple University School of Medicine, 3500 North Broad Street, MERB 1058, Philadelphia, PA 19140. E-mail address: Raghava.Potula@tuhs.temple.edu

The online version of this article contains supplemental material.

Abbreviations used in this paper: ALC, acetyl-L-carnitine; a.u., arbitrary unit; DCF, dichlorodihydrofluorescein; ECM, extracellular medium; ETC, electron transport chain; GSH-px, glutathione peroxidase; METH, methamphetamine; mROS, mitochondrion-derived reactive oxygen species; RNS, reactive nitrogen species; ROS, reactive oxygen species.

www.jimmunol.org/cgi/doi/10.4049/jimmunol.0903691

Materials and Methods

Cells and treatment

PBLs were obtained by countercurrent centrifugal elutriation of leukopheresis packs from HIV-1, 2, and hepatitis B seronegative donors as described previously (22). T cells (>95% anti-CD3$^+$ cells) were isolated from PBL or PBMCs by using a pan-T cell isolation kit according to the manufacturer's protocol (Miltenyi Biotec, Auburn, CA) and separated using an auto-MACS separator. For some experiments, pan-T cells were directly obtained from the Human Immunology Core facility of the University of Pennsylvania. Cell concentration was adjusted to 1×10^6/ml in X-VIVO 20 medium (BioWhitaker, Walkersville, MD) supplemented with 1% heat inactivated normal human serum, 20 μg/ml gentamycin, 2 mM glutamine, and IL-2 (50 U/ml). T cells were exposed to various concentrations of L-methamphetamine hydrochloride (METH, 50 or 100 μM, Sigma-Aldrich, St. Louis, MO) depending on the experiment for different time intervals. Cell viability determined by LIVE/DEAD Fixable Violet Dead Cell Stain Kit (Molecular Probes, Eugene, OR) showed that METH (1–100 μM) had no toxic effects on T cells after 72 h of exposure (Supplemental Fig. 1). Concentrations of METH used in various experiments are based on our pilot experiments that demonstrated the best biological responses and are similar to those of other published studies (6, 17, 23–25) and importantly within the range (≤2–600 μM) found in blood, urine, or tissue samples of METH abusers (26–29).

Reagents and Abs

All chemicals (unless otherwise specified) were purchased from Sigma-Aldrich (St. Lous, MO). The optimal concentration of antioxidants, acetyl-L-carnitine (ALC, 1 mM) and Resveratrol (RES, 8 μM), were determined by preliminary dose-response experiments. These concentrations did not affect cell viability. Antioxidant treatments were initiated 30 min prior to METH application. mAbs against mitochondrial protein complexes (complex I [NADH dehydrogenase] subunit NDUFB8, complex II 30 kDa Ip subunit, 47 kDa complex III core protein 2, complex IV 26 kDa COX subunit II, 55 kDa F_1F_0 ATP synthase [complex V] α subunit, and cytochrome *c*) were obtained from MitoSciences (Eugene, OR). Antinitrotyrosine mAb, clone 1A6, was purchased form Millipore (Billerica, MA).

Calcium measurement

T lymphocytes were affixed to MatTek (Ashland, MA) cell culture dishes coated with Cell-Tak (BD Biosciences, San Jose, CA). T cells were loaded with 10 μM Fluo-4/AM (Invitrogen, Carlsbad, CA) in extracellular medium (ECM) containing 2.0% BSA for 30 min at room temperature. After 1 min of baseline recording, images were acquired every 5 s using the Carl Zeiss 510 Meta confocal microscopy system at 488 excitation. EGTA (0.5 mM) was used to remove extracellular calcium for indicated experiments. The pseudocolorings of the images were done according to the look-up table scale. For simultaneous measurements of cytosolic calcium mobilization and mitochondrial calcium uptake (30), T cells were first loaded with 2 μM Rhod-2/AM (Invitrogen) in ECM at 37°C for 30 min. Rhod-2 loaded cells were washed and loaded with the cytosolic calcium indicator Fluo-4/AM (10 μM) for an additional 30 min at room temperature. T cells were costimulated with anti-CD3 (10 μg)/CD28 (4 μg) and images were acquired after 1 min of baseline recording. The detailed confocal methodology has been published previously (31).

Detection of intracellular ROS

Intracellular ROS were measured by confocal microscopy using the fluorescent probe 2′, 7′-dichlorodihydrofluorescein diacetate (H_2DCFDA, Molecular Probes), which is oxidized to highly fluorescent dichlorodihydrofluorescein (DCF) by ROS. Briefly, T lymphocytes (2×10^6/ml) were incubated with DCF-DA (2 μM) in serum-free X-VIVO 20 medium for 3 h at 37°C in the dark. At the end of incubation, cells were washed and resuspended in 1× HBSS at 37°C. ROS generation was monitored after the addition of METH (100 μM) and detected using the Carl Zeiss 510 Meta confocal microscopy system (Carl Zeiss MicroImaging, Thornwood, NY) at an excitation wavelength of 488 nm. Images were collected in five microscopic fields and fluorescence quantified for three independent experiments using National Institutes of Health ImageJ version 1.42 software (http://rsbweb.nih.gov/ij/). T lymphocytes incubated with 1 mM H_2O_2 for 1 h during DCF staining were used as positive control. BAPTA-AM (25 μM) and MnTBAP (50 μM) were loaded 30 min prior to METH challenge.

Concurrent measurement of cytosolic calcium and mitochondrial-derived ROS production

To visualize mitochondrial-derived ROS (mROS) production, peripheral T cells were loaded with the mitochondrial superoxide sensitive fluorophore, MitoSOX Red (Invitrogen; 10 μM) in ECM containing 2% BSA at 37°C for 20 min. Cells were then incubated with Fluo-4/AM for an additional 20 min at room temperature. At the end of incubation, cells were washed, resuspended in ECM containing 0.25% BSA, and imaged every 5 s at 488 nm and 568 nm for Fluo-4 and MitoSOX Red, respectively. Anti-CD3/CD28 was added after 1 min of baseline recording. Tracings are obtained similarly to those for Fluo-4 and Rhod-2 (30).

Mitochondrial imaging

The changes in mitochondrial membrane potential ($\Delta\psi_m$) were visualized by staining the cells with MitoTracker Red CMXRos (MTR) (Invitrogen). Cells (1×10^6) were incubated with 1 mM MTR to a final concentration of 50 nM in the dark for 30 min at 37°C. The suspension cells were then briefly rinsed with the medium and incubated with all the reagents (METH and valinomycin). The cells were immobilized to Cell-Tak–coated cover slips before analysis by fluorescence microscopy.

Live cell images were obtained under the same acquisition parameters under a ×20 objective for both MitoTracker Red and Hoechst 33342 using a live cell imaging system from Carl Zeiss Microimaging. The live cell imaging system consists of a fully motorized Axio Observer Z1 fluorescent microscope fitted with an AxioCamHR camera and incubator chamber with CO_2 and temperature regulation. After the experimental treatment was initiated, time-lapse image sequences from three different regions in the well were taken at 30 min intervals for 24 h. The average change in intensity over time from the combined images (100–300 cells) was calculated and normalized by setting the initial intensities at t = 0–100%. The results are shown as the average percent intensity ± SEM. The images were analyzed with AxioVision version 4.7 software (Carl Zeiss Microimaging) and with National Institutes of Health ImageJ version 1.42 software (http://rsbweb.nih.gov/ij/).

Flow cytometery

Membrane potential ($\Delta\psi$) was measured by using APO LOGIX JC-1 Assay Kit (Invitrogen). In brief, cells were adjusted to density of 1×10^6 cells/ml and suspended in 0.5 ml of diluted JC-1 reagent according to the manufacturer's instructions. The cells were incubated for 10 min at 37°C in a 5% CO_2 incubator for 15 min in the dark before immediately analyzing them by flow cytometry. Mitochondrial mass (MM) was assessed by using the fluorescent dye, MitoTracker Green FM (MTG; Molecular Probes). Cells were incubated in 0.5 ml PBS containing 100 nM MTG. After incubation for 10 min at 25°C in the dark, samples were immediately transferred to a tube on ice for flow cytometric analysis by LSR II (Becton Dickinson, San Jose, CA). Analysis was carried out using FACS DiVa software (Becton Dickinson).

T cell proliferation and ELISA

Naive T cells with or without METH exposure were stimulated with anti-CD3/CD28. T cells were labeled with 0.5 μM CFSE (BD Pharmingen, San Diego, CA) for 6 min. CFSE intensity was measured by flow cytometry and the proliferative index was calculated with ModFit LT version 2.0 (Verity Software House, Topsham, ME). The proliferation index is a ratio of the sum of the cells in all generations to the computed number of parent cells. Values represent the mean of triplicate determinations in three independent experiments performed with two different cell donors. The IL-2 levels were measured in supernatants after 24 h by ELISA (R&D, Minneapolis, MN) according to the manufacturer's instructions.

Mitochondrial preparations and Western blot analysis

Intact mitochondria from T cells were isolated using a Mitochondria Isolation Kit (MitoScience) according to the manufacturer's instructions. Cells were lysed with CellLytic-M (Sigma-Aldrich) for preparation of whole cell lysate. Protein concentration was measured by BCA assay (Pierce, Rockford, IL). SDS-PAGE and Western blot analysis was performed as previously described (22).

Statistical analysis

Results are presented as mean ± SD and p values < 0.05 are considered significant. Data were analyzed using Prism (GraphPad, La Jolla, CA) and statistical significance for multiple comparisons was assessed by one-way ANOVA with the Newman-Keuls post test.

Results

METH exposure increases cytosolic calcium levels in T cells

Acute METH administration activates dopamine, norepinephrine, and serotonin receptors and inhibits neurotransmitter reuptake,

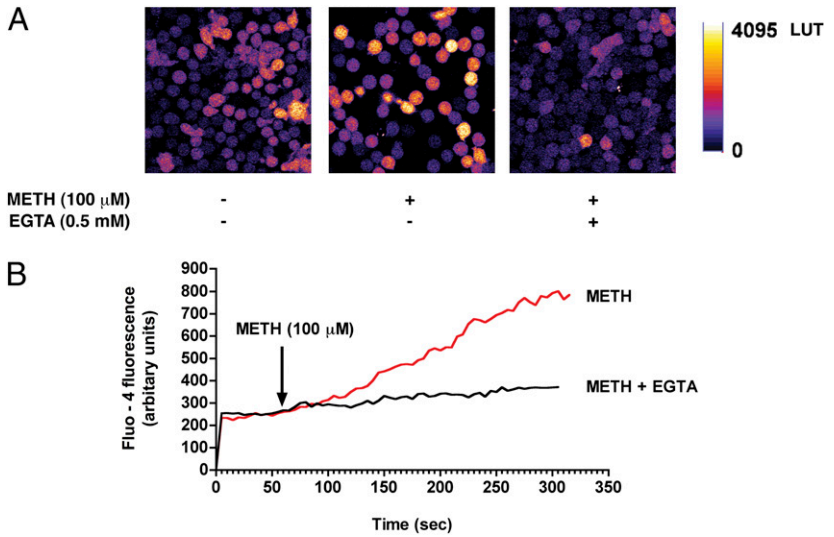

FIGURE 1. METH exposure increases cytosolic calcium levels in T cells. *A*, T cells loaded with the calcium indicator Fluo-4/AM were stimulated with METH (100 μM) and fluorescence changes were imaged via confocal microscopy. Representative pseudocolored images of control and METH-challenged T cells in the presence and absence of the extracellular calcium chelator EGTA (0.5 mM). Original magnification ×600. *B*, Cytosolic calcium levels as detected by Fluo-4 fluorescence following acute exposure to METH (100 μM). $*p < 0.05$ compared with control.

thereby triggering neurotoxicity and cell death (32). METH appears to increase intracellular calcium levels (33, 34) and stimulate ROS generation in both endothelial cells (17) and neurons (35). To date, such effects of METH have not been investigated in T cells. To evaluate whether METH induces a rise in calcium levels in naive T cells, METH at 100 μM was added to T cells and intracellular calcium levels was monitored continuously. We found that METH (100 μM) caused a gradual rise in cytosolic calcium in T lymphocytes as detected by the calcium indicator dye, Fluo-4 (Fig. 1*A*, 1*B*). Because calcium rise occurred gradually, we hypothesized that this elevation in cytosolic calcium originated from the extracellular milieu. Notably, removal of extracellular calcium using the cell-impermeable chelating agent EGTA (0.5 mM) dramatically reduced METH-induced cytosolic calcium levels in T cells (Fig. 1*A*, 1*B*), implicating the increase in calcium was either due to activation of calcium channels or an increase in membrane permeability of mitochondria.

METH-induced calcium increase triggers cellular ROS production

A common target of cytosolic calcium is the mitochondria, resulting in increased cellular bioenergetics and energy production, a by-product of which is the generation of ROS by the mitochondrial respiratory chain (13). T cells exposed to METH (100 μM) elicited a gradual increase in cellular ROS production as detected by the H_2O_2 indicator dye H_2DCF-DA (Fig. 2*A*). To assess the contribution of calcium to cellular ROS production, T cells were preincubated with the calcium chelator BAPTA-AM (25 μM). Removal of intracellular calcium attenuated METH-induced ROS generation (Fig. 2*B*, 2*C*). Similarly, ROS production after METH

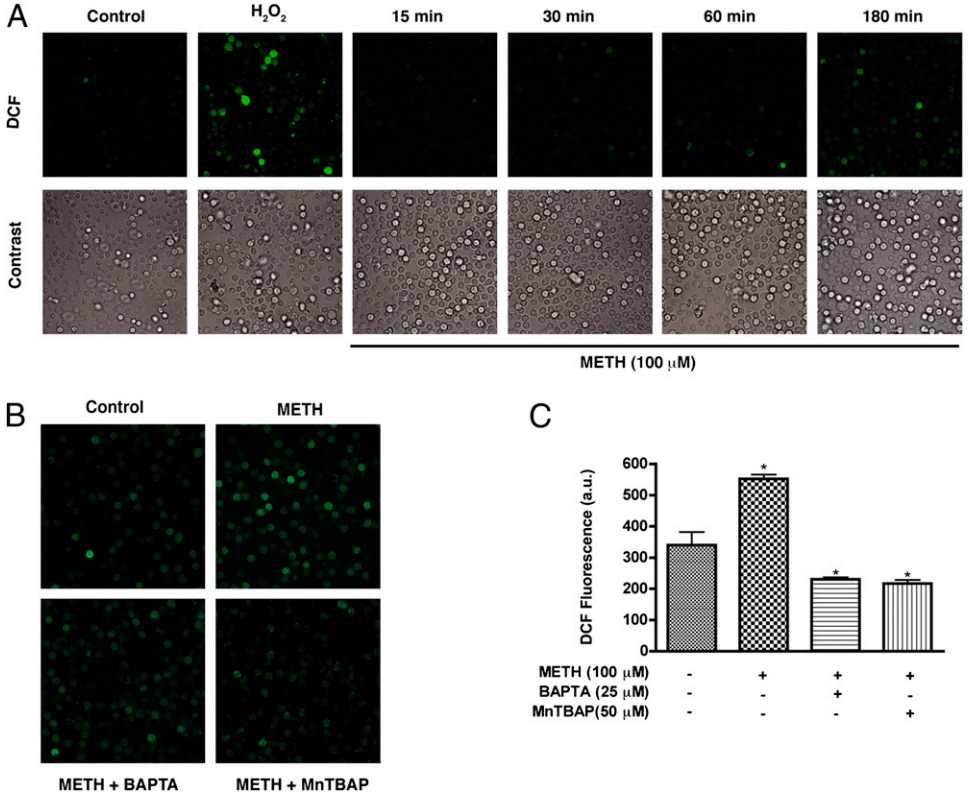

FIGURE 2. METH-induced calcium increase triggers cellular ROS production. *A*, T cells loaded with the H_2O_2 indicator dye H_2DCF-DA were exposed to METH (100 μM) for varying time points. H_2O_2 (1 μM) was incubated with T cells for 20 min as a positive control. *B*, H_2DCF-DA–loaded T cells were incubated with the intracellular calcium chelator BAPTA-AM (25 μM) or the ROS scavenger MnTBAP (50 μM) for 1 h prior to METH exposure. Original magnification ×200. *C*, Quantification of DCF fluorescence (a.u.) of five microscopic fields from three independent experiments. a.u., arbitrary unit.

exposure was decreased by incubation of T cells with the mitochondrial antioxidant MnTBAP (50 μM) (Fig. 2*B*, 2*C*). Taken together, these data indicate that mitochondria are a major source of ROS after exposure.

Impaired calcium mobilization in T cells exposed to METH triggers mROS

Stimulation of T cells through TCRs initiates a coordinated cascade of signaling events, which ultimately initiate a synchronized program of activation, proliferation, and differentiation. Because one of the key signaling events triggered by TCR engagement is the elevation of cytoplasmic calcium concentration, we considered investigating whether METH exposure affects TCR-CD28 dependent calcium mobilization. To this end, human peripheral T cells exposed to METH (100 μM) were loaded with Fluo-4 and Rhod-2 for simultaneous measurement of cytoplasmic and mitochondrial calcium levels, respectively. Surprisingly, CD3/CD28 costimulation-induced cytosolic calcium levels in control and METH-treated T cells were not significantly different (Fig. 3*A*). In contrast, compared with the control cells, METH-exposed cells showed a sustained elevation of mitochondrial calcium in response to anti-CD3/CD28 stimulation (Fig. 3*B*). These data suggest that the discordance between the levels of cytosolic and mitochondrial calcium in T cells exposed to METH is attributable to mitochondrial calcium handling capacity. Furthermore, because the foremost feature of mitochondrial functional alterations is the production of ROS (36, 37), we considered whether receptor-mediated calcium signals that are transmitted to the mitochondria might in turn lead to mROS

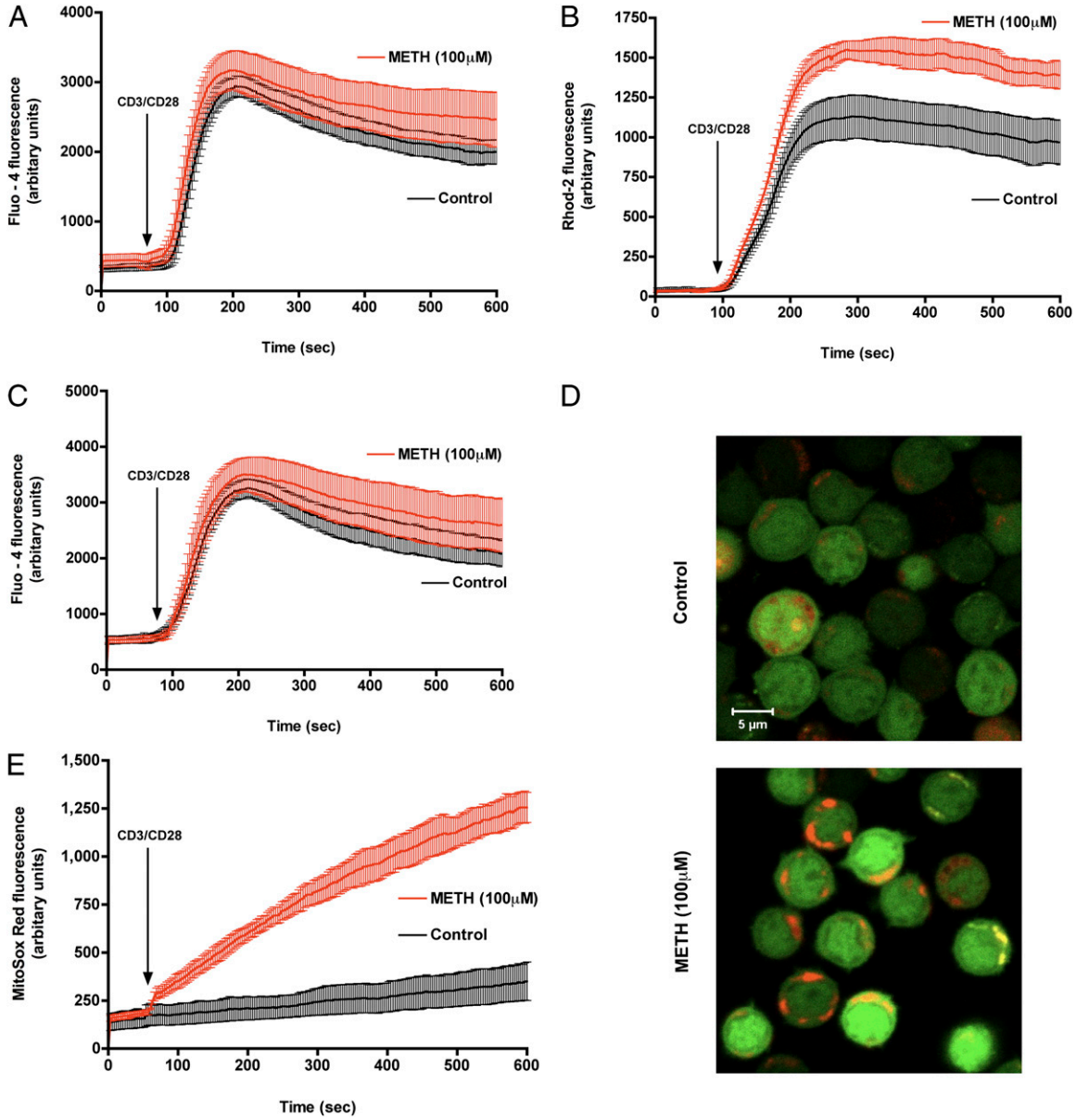

FIGURE 3. METH exposure augments CD3/CD28-evoked mitochondrial calcium uptake and mROS production. Representative traces of control (black) and METH-treated T cells (red) displaying (*A*) cytosolic calcium and (*B*) mitochondrial calcium levels after CD3/CD28 costimulation. *C*, Control and METH-exposed T cells loaded with the cytosolic calcium indicator Fluo-4/AM (green) and the mitochondrial calcium indicator Rhod-2 (red) were stimulated with anti-CD3/CD28. Time-lapse confocal microscopy revealed sustained mitochondrial calcium levels in cells pretreated with METH. *D*, Representative pseudocolored images of T cells either left untreated (*top*) or exposed for 3 h to METH (*bottom*) were loaded with the mitochondrion-derived superoxide indicator, MitoSOX Red, and imaged by confocal microscopy. Original magnification ×600. *E*, Quantitation of mROS production in live T cells. METH-treated cells, but not control cells, displayed sustained mROS production.

generation. Control and METH-treated T cells were loaded with the cytoplasmic calcium indicator dye, Fluo-4 and the mROS indicator MitoSOX Red (31, 38) to simultaneously assess the cytosolic calcium and mROS generation in response to CD3/CD28 costimulation. MitoSOX Red is nonfluorescent until oxidized by superoxide, and an increase in the fluorescence of MitoSOX Red indicates oxidation by mitochondrial superoxide. For instance, inhibition of normal cytochrome electron transport by antimycin A (Supplemental Fig. 2) exacerbated mROS production in T cells. A synergistic increase in mROS was noted in METH-treated T cells response to CD3/CD28 costimulation (Fig. 3*D*, 3*E*) compared with control, whereas simultaneous cytoplasmic calcium levels measured by Fluo-4 remained unaffected (Fig. 3*C*). These observations indicate that the inability of the METH-exposed T cell to maintain mitochondrial calcium homeostasis on CD3/CD28 costimulation contributes to mROS production. Taken together, the data suggest that METH exposure triggers mROS production that is facilitated by mitochondrial calcium uptake.

Effects of METH on T cell mitochondria

The $\Delta\psi_m$ represents a primary indicator of membrane stability in mitochondria (39). Elevated mROS and altered mitochondrial calcium handling have been shown to directly facilitate mitochondrial dysfunction (40). Because mROS is an important regulator of $\Delta\psi_m$ and maintenance of the $\Delta\psi_m$ is important for oxidative phosphorylation activity, a decrease would result in mitochondrial dysfunction, we therefore sought to assess whether membrane potential is an early indicator of METH effects on T cells. Cells were loaded with MTR, which labels mitochondria in live cells, and its decrease in intensity is indicative of a lowering in membrane potential. As shown in Fig. 4*A* and 4*B*, the mitochondrial membrane potential dropped 40% after 6 h exposure in a time-dependent manner ($p < 0.05$). In addition, quantitative estimation of $\Delta\psi_m$ was also performed using a different dye, JC-1. Loss in $\Delta\psi_m$ was detected as a shift in fluorescence from red to green in cells (Fig. 4*C*) and was documented as early as 30 min after METH treatment, indicating diminished JC-1 accumulation in the mitochondrial matrix. More-

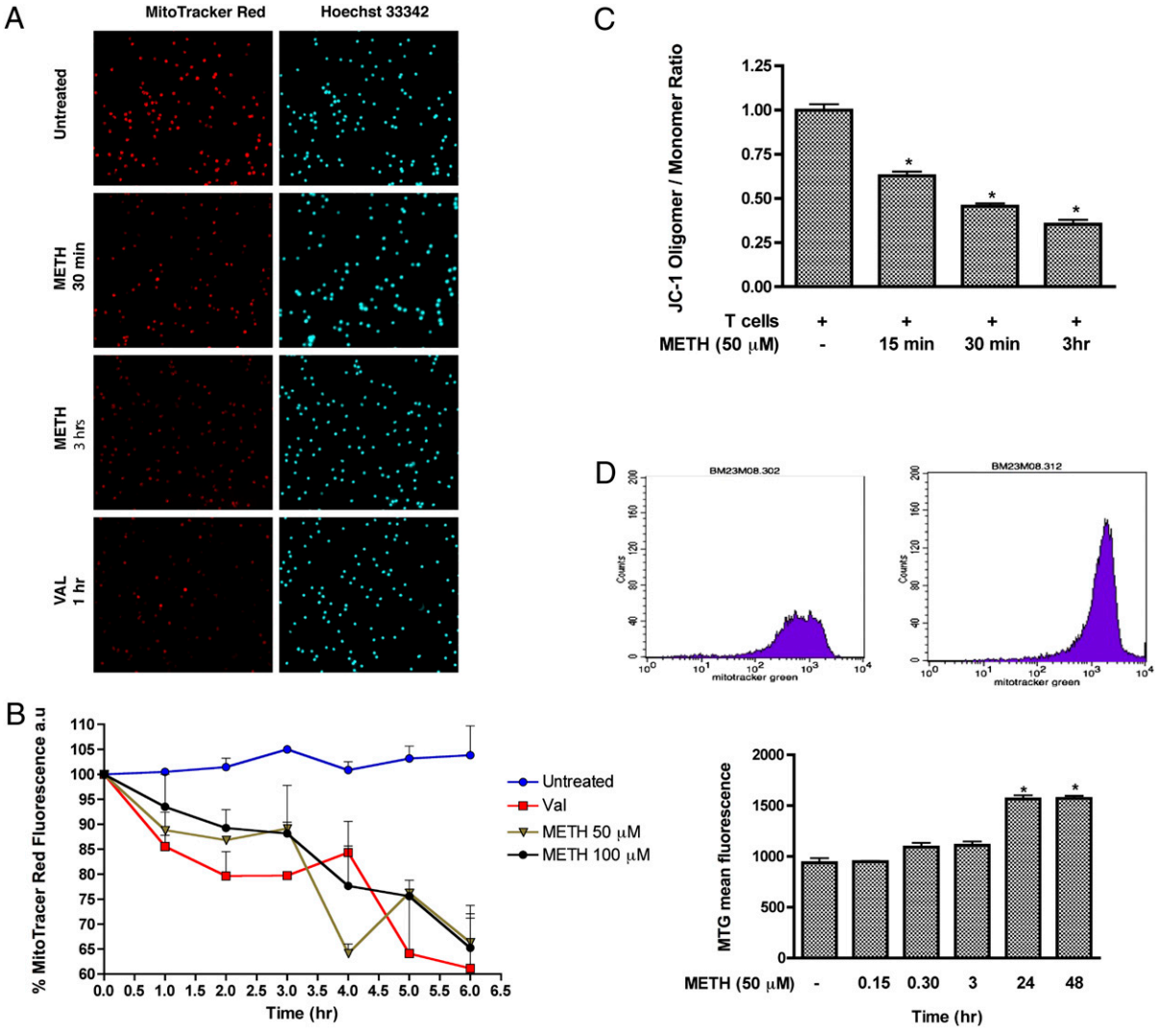

FIGURE 4. METH induces loss of mitochondrial membrane potential in T cells**.** *A*, Visualization of mitochondrial membrane potential by MTR. Representative photomicrographs of MTR (red), and Hoechst nuclear staining (blue). Original magnification ×200. *B*, Quantitative analysis of MTR. *C*, Graphical representation of red fluorescence (Oligomer; FL2) versus green fluorescence (Monomer; FL1) ratio representing the mitochondrial membrane potential using JC-1. *D*, Data represent the mean values ± SD from experiments performed in triplicate. All images were acquired at the same exposure time. *Designates a significant decrease ($p < 0.05$) compared with T cells treated with METH alone. *D,* Representative histogram depicting MTG fluorescence in T cells. Untreated T cells and T cells treated with METH for 24 h are shown. Statistical analysis of three independent experiments with $*p < 0.05$ compared with the untreated sample.

over, after 3 h exposure, the fluorescence intensity was further diminished (>60%; $p < 0.05$). Next, to determine whether METH could cause changes in the amount of mitochondria, we used the fluorescent mitochondrial specific dye, MTG, to monitor MM. In this assay, the dye binds to the mitochondrial membrane independent of membrane potential and staining intensity indicates MM (41–44). T cells were treated with the indicated concentrations of METH (50 μM) for 0–48 h and the mean fluorescence intensity was measured. At 24–48 h, the MTG intensity of METH-exposed cells was 1.7-fold higher as compared with control untreated cells ($p < 0.05$, Fig. 4*D*). Based on these results, it is plausible to suggest that METH treatment at early time leads to mitochondrial injury and later results in mitochondrial swelling or an increase in the number of mitochondria (evidenced by higher MTG intensity).

METH exposure increases cellular nitrosylation in T cells

NO generated during ROS production reacts to form the strong oxidizing agent peroxynitrite. Peroxynitrite in turn can modify tyrosine residues in a process known as nitration, which has been implicated in cellular damage in several pathologic conditions. We assessed nitrosylation of protein in whole cell lysate by immunoblotting of protein extracts obtained from control and T cells exposed to METH. The nitrotyrosine level in METH-treated T cells increased significantly within 15–30 min of treatment when compared with control cells ($p < 0.01$, Fig. 5). These results suggest that METH exposure caused production of strong oxidants, which can modify protein residues (tyrosine nitration), which can lead to impaired cellular enzymes, membranes, and organelles.

Mitochondrial protein content is altered in METH-treated T cells

A compromise of cellular redox homeostasis results in oxidative stress. The imbalance may be either due to overproduction of ROS or to a deficiency in antioxidant defense mechanisms. Because primary sites for mROS production are the enzyme complexes of the ETC (45), we investigated whether levels of these mitochondrial proteins were altered after METH treatment. Immunoblot analysis of the mitochondrial fraction from T cells treated with METH revealed a notable decrease in protein levels of complexes I (subunit NDUFB8), III (core protein 2), and IV (subunit II) of the ETC (Fig. 6). We did not detect appreciable change in the protein content of complex II (Ip subunit), complex V (α subunit), or cytochrome *c*. Importantly, pretreatment of T cells with three different antioxidants was able to prevent the reduction of complexes I, III, and IV proteins after METH exposure.

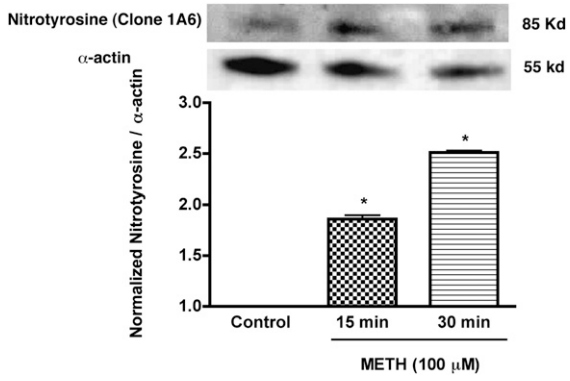

FIGURE 5. Enhanced expression of nitrotyrosine in T cells treated with METH. Western blot analysis of nitrotyrosine levels of METH (100 μM) treated and untreated T cells. Representative immunoblots of nitrotyrosine and internal standard α-actin are shown in blots and the ratios of nitrotyrosine staining to α-actin are shown in the histogram. Error bars represent mean ± SD of three independent experiments. $*p < 0.01$ (METH treated versus control).

METH causes suppression of T cell proliferative responses and inhibits IL-2 secretion

Oxidative stress impairs several T cell functions, including decreased production of cytokines and reduced capacity of lymphocytes to respond to relevant stimuli as shown in several diseases (19–21, 46). Because METH abuse has been shown to impair immunological functions (1, 2, 4, 47), we sought to evaluate how METH-induced ROS could affect T cell functions (IL-2 production and T cell proliferation). As a prelude to measuring T cell function after METH treatment, we examined the proliferative response of T cells costimulated with CD3/CD8 in the presence or absence of METH. The proliferative index of cells treated with METH was significantly reduced (21%, $p < 0.001$) as compared with control (Fig. 7*A*). T cells activated in similar fashion showed enhanced secretion of IL-2, and METH treatment resulted in 3-fold reduction of IL-2 levels ($p < 0.01$, Fig. 7*B*). We next evaluated whether the effect of METH on IL-2 via generation of reactive species could be reversed by antioxidants. Pretreatment of T cells with antioxidants prior to METH treatment restored production of IL-2 (Fig. 7*B*).

Discussion

In recent years, considerable progress has been made in delineating the immunosuppressive effects of METH, a substance that is abused by 35 million people worldwide (48). Nevertheless, little is known about the oxidative and immunotoxic effects of METH on T cells as a potential mechanism of METH-mediated immune suppression. In the current study, we show for the first time that METH alters intracellular calcium mobilization in T cells, leading to subsequent generation of ROS, which correlates with mitochondrial damage and leads to impaired T cell function. The role of oxidative stress in the etiology of numerous human diseases has been clearly demonstrated (49–52). Experimental and clinical data point toward mitochondrial oxidative damage and dysfunction as important contributors to a number of pathologic conditions associated with METH abuse (53, 54). However, the mechanism by which METH-induced oxidative stress contributes to cellular dysfunction is poorly understood.

The mitochondrion serves as the primary source of both intracellular ROS and ATP production, a process governed by the second messenger, calcium. Extracellular stimuli initiate cellular signaling via an increase in intracellular calcium (55), which is readily sequestered by mitochondria. On mitochondrial entry, calcium enhances the activity of the tricarboxylic acid cycle dehydrogenases (56), rapidly elevating cellular levels of the mitochondrial complex I substrate, NADH, to stimulate energy production (57). This rapid increase in mitochondrial respiration saturates complex I and promotes electron leakage at complex III, which reacts with molecular oxygen to form ROS (58). Although long considered a simple byproduct of increased respiration, it is now appreciated that physiologic mROS generation serves to integrate energy production with energy demand by indicating the availability of sufficient metabolic substrates for T cell proliferation (11). As important secondary messengers, ROS act as mediators of immunity; however, ROS overproduction can impair T cell responses (59). In the striatum by mechanisms not completely understood, METH increases cytosolic calcium levels most likely at the plasma membrane via the extracellular milieu, initiating production of ROS and cell death in brain tissue (60). Because of the known immunotoxic effect of METH on T cells, we tested the idea that METH-mediated calcium elevations lead to increased generation of ROS and reactive RNS, which in turn trigger mitochondrial oxidative

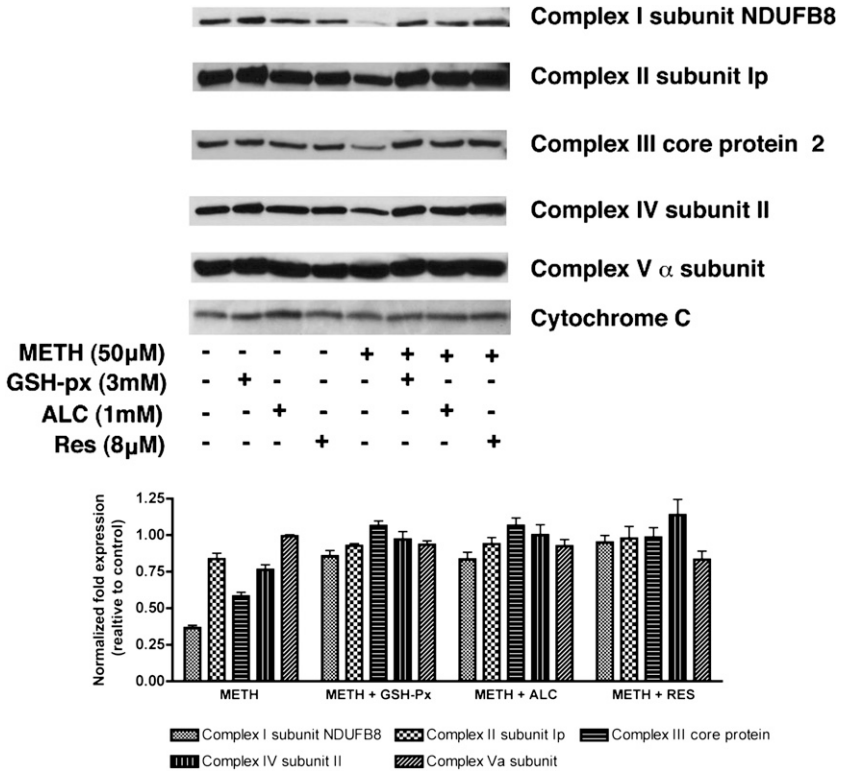

FIGURE 6. Changes in expression of specific mitochondrial protein in T cells in response to METH. Primary human T cells either pretreated (30 min) with antioxidants as indicated or untreated were exposed to METH (50 μM). Representative immunoblots of three independent experiments and the relative fold expression of protein subunits normalized to cytochrome *c* are shown in the histogram. The corresponding complexes of the specific subunits are indicated in parentheses. After 24 h, cells were harvested, and the mitochondrial fraction of the cell was isolated according to the protocol provided by the manufacturer (MitoSciences). Equal amounts of mitochondrial protein were analyzed by SDS-PAGE and immunoblotted with Abs to complex I (NADH dehydrogenase) subunit NDUFB8, complex II 30 kDa Ip subunit, 47 kDa complex III core protein 2, complex IV 26 kDa COX subunit II, 55 kDa F_1F_0 ATP synthase (complex V) α subunit, or cytochrome *c* (MitoSciences). Pretreatment with antioxidants (GSH-px, ALC, and RES) 30 min prior to METH exposure appreciably prevented alteration of protein content of mitochondrial respiratory complexes I, III, and IV. GSH-px, glutathione peroxidase.

damage and dysfunction. Our data indicated that METH increased cellular calcium entry that corresponded to an increase in intracellular ROS levels, and a calcium chelator in the media prevented these changes. Interestingly, we found that although cytosolic calcium levels remained significantly unaltered in METH-treated T cells in response to CD3/CD28 costimulation (Fig. 3*A*), the mitochondrial calcium uptake level measured by Rhod-2 was significantly increased (Fig. 3*B*). We reasoned that the observed discordance between unaltered cytosolic calcium levels and increased mitochondrial calcium uptake in T cells exposed to METH is attributable to mitochondrial calcium handling capacity, resulting in mitochondrial calcium overload that leads to mROS generation. Indeed, the basis for this observed discordance was supported by simultaneous assessment of cytoplasmic calcium levels (Fig. 3*C*, 3*D*) and generation of mitochondrial superoxide (Fig. 3*D*, 3*E*).

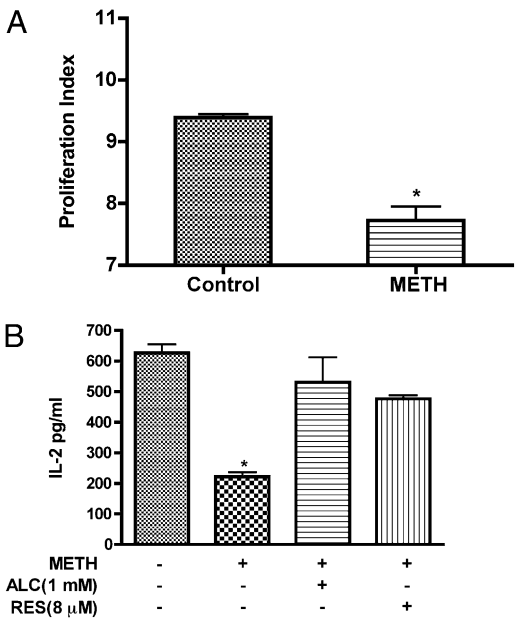

FIGURE 7. METH suppresses T cell proliferation and IL-2 secretion. *A*, Freshly isolated T cells labeled with CFSE were stimulated with anti-CD3/CD28 in the absence or presence of METH (50 μM). In contrast to untreated cells, on TCR engagement, METH-treated T cells showed decreased T cell proliferation (*$p < 0.001$). *B*, T cells were stimulated with anti-CD3/CD28 for 24 h and supernatant fluid was analyzed for IL-2 production by ELISA. *Designates significant decrease ($p < 0.01$) compared with nontreated T cells.

The $\Delta\psi_m$ assures major bioenergetic function of the mitochondrion; $\Delta\psi_m$ collapse as a response to extraneous environmental stimuli contributes to the loss of cellular functions (61, 62). To investigate the effects of METH exposure on T cells, we measured $\Delta\psi_m$ using two-mitochondrial probes, MTR and a fluorescent cationic dye, JC-1 that effectively detect change in membrane potential. MTR binds covalently to thiol residues of mitochondrial proteins, depending on the electrical potential of the organelles. The lipophilic dye JC-1 in healthy cells with an intact $\Delta\psi_m$ interacts with the mitochondrial matrix and once the critical concentration is exceeded, form aggregates, which stains the mitochondria red. In conditions where there is a decrease in $\Delta\psi_m$, the dye leaks from the mitochondria, remains in its monomeric form, and appears green. Furthermore, because the positive charge and lipophilic nature of the METH cation allows its diffusion into mitochondria where it is retained by these organelles (63), could further facilitate the time-dependent loss in $\Delta\psi_m$ in T cells after METH treatment.

Another indicator of mitochondrial impairment was a significant time-dependent increase in MM in T cells ater 24–48 h exposure to METH (Fig. 4*D*). In comparison with untreated cells, MTG fluorescence was increased in T cells treated with METH. These data are consistent with recent findings of augmented MM seen in human neurobalstoma cells during METH treatment (64). The increase of MM could be viewed as a compensatory mechanism that may represent enhanced mitochondrial biogenesis in METH-treated T cells. Alternatively, as mitochondria constitute major Ca^{2+} stores (65), increased MM may account for altered Ca^{2+}

handling in cells exposed to METH. Such changes may be an important adaptive cellular mechanism aiming to reduce oxidative stress without a necessary alteration in respiration and energy supply (66, 67). However, one cannot distinguish by flow cytometry-based assay whether high MM corresponds to higher numbers of mitochondria or larger organelles, both resulting in more intense staining. Further experiments using electron microscopy are needed to clarify this issue. A number of oxidative and nitrative modifications occur in proteins as a result of oxidative damage (68–70). To date, it is to be determined whether this relationship is causative or simply correlative. Nevertheless, the studies of these protein modifications serve as important molecular biomarkers of oxidative/nitrosative damage and contribute to the establishment of a relationship between the insult and protein structural and functional changes (71, 72). In the current study, the increased production of nitrotyrosine reflects oxidative stress in T cells mediated by METH. Consistent with our data, oxidative damage of proteins, lipids, and DNA was reported in response to repeated METH administration (43, 73). The rapid generation of ROS/RNS on METH exposure probably affects the antioxidant capacity of T cells, rendering them unable to keep up with radical production and initiating the oxidative modification of proteins.

The ability of lymphocytes to proliferate and differentiate into effector cells in response to antigenic stimuli is essential for generation of a robust adaptive immune response (74). Therefore, T cell proliferation in response to a stimulus is an appropriate indicator for cellular immunity. We demonstrate in this study that exposure of T cells to METH results in the loss of T cell proliferative activity. Previous studies have indicated that ROS could prevent proliferation of T lymphocytes and production of key cytokines and effector molecules thereby orchestrating immune responses (59, 75). These changes, coupled with the METH-induced direct immunosuppressive effects on dendritic cells and macrophages (48), suggest that METH has multifaceted effects on different arms of immunity. The finding that oxidative stress may be a forerunner for loss in T cell function due to METH abuse could have far-reaching implications not just for the induction of immune response, but also for other processes (such as generation of antigenic peptides and cell cycle regulation) that are important for immune regulation.

ROS are both produced within T cells and are released into the extracellular space at varying concentrations. At physiological levels, ROS are involved in T cell signaling and maintain homeostasis (76). At higher levels, ROS are toxic and have detrimental effects on the cells. The results from our current study demonstrate that mitochondria are both a source and a target for ROS. Consistent with our findings, an increase in oxidative stress due to METH or its metabolites has been reported (41, 42, 61, 64, 73). Moreover, previous studies have suggested a role for the mitochondrial ETC in mediating toxicity of METH (77). The outer and inner membranes and electron transport chain complexes of the mitochondria play a pivotal role in regulation of energy production. The major source of mROS production is the ubiquinone sites of the respiratory chain enzymes of complexes I (NADH-dehydrogenase) and III (45). METH exposure of human T lymphocytes resulted in reduced expression of complex I (NADH dehydrogenase) subunit NDUFB8, complex III (ubiquinol cytochrome *c* oxidoreductase) subunit core protein 2, and complex IV (Cox II). Similar findings of decreased protein expression of mitochondrial respiratory complexes were reported in rat brain (78) and human neuroblastoma cells (64) after METH treatment. ROS production is significantly enhanced if electron transport is altered through these complexes due to subtle changes in the expression of these subunits (79). It is therefore plausible to conceive that the chronic increase in ROS production in response to METH may be due to modifications in mitochondrial complex proteins (especially complex I and III), which promote inefficient electron flow through the respiratory chain and subsequent ROS generation. Based on these findings, we conclude that acute ROS production in response to METH is due to the rise in cytosolic calcium and saturation of the ETC, which leads to the oxidative modification of proteins and mitochondrial dysfunction. Chronically, METH-induced ROS production leads to a compensatory downregulation of mitochondrial proteins that, while protecting T cells from ROS during acute METH exposure, may affect long-term cellular redox balance and the ability of T cells to respond to pathogens. Similarly, the loss of intracellular ATP levels in T cells treated with METH (Supplemental Fig. 3) provides additional support for the hypothesis that METH-mediated ROS production consequently results in mitochondria dysfunction.

Antioxidants are pivotal in maintaining redox balance by either preventing the formation of free radicals, detoxifying them, or by scavenging the reactive species or their precursors. The broad spectrum of biological functions of the antioxidants suggests the existence of multiple molecular targets that mediate diverse responses, best understood in the context of their clinical and biochemical effects on reactive species. ALC, an acetylated derivative of L-carnitine, exhibits the antioxidant defense through both improved β-oxidation and direct oxygen radical scavenging activity. Phenolic antioxidants, such as RES, act by preventing lipid peroxidation of membrane polyunsaturated fatty acids thus preventing loss of membrane integrity. GHS-px, an enzyme functions as a primary endogenous antioxidant by preventing ROS formation (80). Importantly, antioxidants with diverse modes of action prevented METH-induced ROS generation, its inhibitory effects on mitochondrial complex I, III, and IV expression and the decreased IL-2 production by METH-exposed T cell. Our data suggest that mitochondrial oxidative damage is responsible for METH-mediated toxicity and that antioxidant application can protect this organelle and the cell from toxic injury.

In summary, our data suggest that an important target of METH-induced cellular ROS in naive and activated T cells is the mitochondrion, resulting in mitochondrial injury (decreased membrane potential and increased MM). The ensuing METH-induced generation of ROS represents a redox-dependent pathway mediating T cell immune dysfunction.

Disclosures

The authors have no financial conflicts of interest.

References

1. Iwasa, H., S. Kikuchi, S. Hasegawa, K. Suzuki, and T. Sato. 1996. Alteration of G protein subclass mRNAs in methamphetamine-induced behavioral sensitization. *Ann. N. Y. Acad. Sci.* 801: 110–115.
2. Zule, W. A., and D. P. Desmond. 1999. An ethnographic comparison of HIV risk behaviors among heroin and methamphetamine injectors. *Am. J. Drug Alcohol Abuse* 25: 1–23.
3. Phillips, T. R., J. N. Billaud, and S. J. Henriksen. 2000. Methamphetamine and HIV-1: potential interactions and the use of the FIV/cat model. *J. Psychopharmacol. (Oxford)* 14: 244–250.
4. Yu, Q., D. Zhang, M. Walston, J. Zhang, Y. Liu, and R. R. Watson. 2002. Chronic methamphetamine exposure alters immune function in normal and retrovirus-infected mice. *Int. Immunopharmacol.* 2: 951–962.
5. In, S. W., E. W. Son, D. K. Rhee, and S. Pyo. 2005. Methamphetamine administration produces immunomodulation in mice. *J. Toxicol. Environ. Health A* 68: 2133–2145.
6. Mahajan, S. D., Z. Hu, J. L. Reynolds, R. Aalinkeel, S. A. Schwartz, and M. P. Nair. 2006. Methamphetamine modulates gene expression patterns in monocyte derived mature dendritic cells: implications for HIV-1 pathogenesis. *Mol. Diagn. Ther.* 10: 257–269.
7. Saito, M., M. Terada, T. Kawata, H. Ito, N. Shigematsu, P. Kromkhun, M. Yokosuka, and T. R. Saito. 2008. Effects of single or repeated administrations of methamphetamine on immune response in mice. *Exp. Anim.* 57: 35–43.
8. Nair, M. P., Z. M. Saiyed, N. Nair, N. H. Gandhi, J. W. Rodriguez, N. Boukli, E. Provencio-Vasquez, R. M. Malow, and M. J. Miguez-Burbano. 2009. Metham-

phetamine enhances HIV-1 infectivity in monocyte derived dendritic cells. *J. Neuroimmune Pharmacol.* 4: 129–139.
9. Martinez, L. R., M. R. Mihu, A. Gácser, L. Santambrogio, and J. D. Nosanchuk. 2009. Methamphetamine enhances histoplasmosis by immunosuppression of the host. *J. Infect. Dis.* 200: 131–141.
10. Jekabsons, M. B., and D. G. Nicholls. 2004. In situ respiration and bioenergetic status of mitochondria in primary cerebellar granule neuronal cultures exposed continuously to glutamate. *J. Biol. Chem.* 279: 32989–33000.
11. Jones, R. G., T. Bui, C. White, M. Madesh, C. M. Krawczyk, T. Lindsten, B. J. Hawkins, S. Kubek, K. A. Frauwirth, Y. L. Wang, et al. 2007. The proapoptotic factors Bax and Bak regulate T Cell proliferation through control of endoplasmic reticulum Ca(2+) homeostasis. *Immunity* 27: 268–280.
12. Quintana, A., C. Schwindling, A. S. Wenning, U. Becherer, J. Rettig, E. C. Schwarz, and M. Hoth. 2007. T cell activation requires mitochondrial translocation to the immunological synapse. *Proc. Natl. Acad. Sci. USA* 104: 14418–14423.
13. Hawkins, B. J., L. A. Solt, I. Chowdhury, A. S. Kazi, M. R. Abid, W. C. Aird, M. J. May, J. K. Foskett, and M. Madesh. 2007. G protein-coupled receptor Ca2+-linked mitochondrial reactive oxygen species are essential for endothelial/leukocyte adherence. *Mol. Cell. Biol.* 27: 7582–7593.
14. D'Aurelio, M., M. Merlo Pich, L. Catani, G. L. Sgarbi, C. Bovina, G. Formiggini, G. Parenti Castelli, H. Baum, S. Tura, and G. Lenaz. 2001. Decreased Pasteur effect in platelets of aged individuals. *Mech. Ageing Dev.* 122: 823–833.
15. Fukami, G., K. Hashimoto, K. Koike, N. Okamura, E. Shimizu, and M. Iyo. 2004. Effect of antioxidant N-acetyl-L-cysteine on behavioral changes and neurotoxicity in rats after administration of methamphetamine. *Brain Res.* 1016: 90–95.
16. Stephans, S. E., and B. K. Yamamoto. 1994. Methamphetamine-induced neurotoxicity: roles for glutamate and dopamine efflux. *Synapse* 17: 203–209.
17. Ramirez, S. H., R. Potula, S. Fan, T. Eidem, A. Papugani, N. Reichenbach, H. Dykstra, B. B. Weksler, I. A. Romero, P. O. Couraud, and Y. Persidsky. 2009. Methamphetamine disrupts blood-brain barrier function by induction of oxidative stress in brain endothelial cells. *J. Cereb. Blood Flow Metab.* 29: 1933–1945.
18. Grisham, M. B. 2004. Reactive oxygen species in immune responses. *Free Radic. Biol. Med.* 36: 1479–1480.
19. Stefanová, I., M. W. Saville, C. Peters, F. R. Cleghorn, D. Schwartz, D. J. Venzon, K. J. Weinhold, N. Jack, C. Bartholomew, W. A. Blattner, et al. 1996. HIV infection—induced posttranslational modification of T cell signaling molecules associated with disease progression. *J. Clin. Invest.* 98: 1290–1297.
20. Zea, A. H., M. T. Ochoa, P. Ghosh, D. L. Longo, W. G. Alvord, L. Valderrama, R. Falabella, L. K. Harvey, N. Saravia, L. H. Moreno, and A. C. Ochoa. 1998. Changes in expression of signal transduction proteins in T lymphocytes of patients with leprosy. *Infect. Immun.* 66: 499–504.
21. Maurice, M. M., A. C. Lankester, A. C. Bezemer, M. F. Geertsma, P. P. Tak, F. C. Breedveld, R. A. van Lier, and C. L. Verweij. 1997. Defective TCR-mediated signaling in synovial T cells in rheumatoid arthritis. *J. Immunol.* 159: 2973–2978.
22. Potula, R., S. H. Ramirez, B. Knipe, J. Leibhart, K. Schall, D. Heilman, B. Morsey, A. Mercer, A. Papugani, H. Dou, and Y. Persidsky. 2008. Peroxisome proliferator-activated receptor-gamma activation suppresses HIV-1 replication in an animal model of encephalitis. *AIDS* 22: 1539–1549.
23. Maragos, W. F., K. L. Young, J. T. Turchan, M. Guseva, J. R. Pauly, A. Nath, and W. A. Cass. 2002. Human immunodeficiency virus-1 Tat protein and methamphetamine interact synergistically to impair striatal dopaminergic function. *J. Neurochem.* 83: 955–963.
24. Theodore, S., W. A. Cass, A. Nath, J. Steiner, K. Young, and W. F. Maragos. 2006. Inhibition of tumor necrosis factor-alpha signaling prevents human immunodeficiency virus-1 protein Tat and methamphetamine interaction. *Neurobiol. Dis.* 23: 663–668.
25. Reynolds, J. L., S. D. Mahajan, D. E. Sykes, S. A. Schwartz, and M. P. Nair. 2007. Proteomic analyses of methamphetamine (METH)-induced differential protein expression by immature dendritic cells (IDC). *Biochim. Biophys. Acta* 1774: 433–442.
26. Melega, W. P., A. K. Cho, D. Harvey, and G. Laćan. 2007. Methamphetamine blood concentrations in human abusers: application to pharmacokinetic modeling. *Synapse* 61: 216–220.
27. Kalasinsky, K. S., T. Z. Bosy, G. A. Schmunk, G. Reiber, R. M. Anthony, Y. Furukawa, M. Guttman, and S. J. Kish. 2001. Regional distribution of methamphetamine in autopsied brain of chronic human methamphetamine users. *Forensic Sci. Int.* 116: 163–169.
28. Klette, K. L., A. R. Kettle, and M. H. Jamerson. 2006. Prevalence of use study for amphetamine (AMP), methamphetamine (MAMP), 3,4-methylenedioxyamphetamine (MDA), 3,4-methylenedioxy-methamphetamine (MDMA), and 3,4-methylenedioxy-ethylamphetamine (MDEA) in military entrance processing stations (MEPS) specimens. *J. Anal. Toxicol.* 30: 319–322.
29. Takayasu, T., T. Ohshima, J. Nishigami, T. Kondo, and T. Nagano. 1995. Screening and determination of methamphetamine and amphetamine in the blood, urine and stomach contents in emergency medical care and autopsy cases. *J. Clin. Forensic Med.* 2: 25–33.
30. Madesh, M., W. X. Zong, B. J. Hawkins, S. Ramasamy, T. Venkatachalam, P. Mukhopadhyay, P. J. Doonan, K. M. Irrinki, M. Rajesh, P. Pacher, and C. B. Thompson. 2009. Execution of superoxide-induced cell death by the pro-apoptotic Bcl-2-related proteins Bid and Bak. *Mol. Cell. Biol.* 29: 3099–3112.
31. Mukhopadhyay, P., M. Rajesh, G. Haskó, B. J. Hawkins, M. Madesh, and P. Pacher. 2007. Simultaneous detection of apoptosis and mitochondrial superoxide production in live cells by flow cytometry and confocal microscopy. *Nat. Protoc.* 2: 2295–2301.
32. Cadet, J. L., I. N. Krasnova, S. Jayanthi, and J. Lyles. 2007. Neurotoxicity of substituted amphetamines: molecular and cellular mechanisms. *Neurotox. Res.* 11: 183–202.
33. Uramura, K., T. Yada, S. Muroya, and M. Takigawa. 2000. Ca2+ oscillations in response to methamphetamine in dopamine neurons of the ventral tegmental area in rats subchronically treated with this drug. *Ann. N. Y. Acad. Sci.* 914: 316–322.
34. Goodwin, J. S., G. A. Larson, J. Swant, N. Sen, J. A. Javitch, N. R. Zahniser, L. J. De Felice, and H. Khoshbouei. 2009. Amphetamine and methamphetamine differentially affect dopamine transporters in vitro and in vivo. *J. Biol. Chem.* 284: 2978–2989.
35. Tata, D. A., and B. K. Yamamoto. 2007. Interactions between methamphetamine and environmental stress: role of oxidative stress, glutamate and mitochondrial dysfunction. *Addiction* 102(Suppl 1): 49–60.
36. Turrens, J. F. 2003. Mitochondrial formation of reactive oxygen species. *J. Physiol.* 552: 335–344.
37. Murphy, M. P. 2009. How mitochondria produce reactive oxygen species. *Biochem. J.* 417: 1–13.
38. Mukhopadhyay, P., M. Rajesh, K. Yoshihiro, G. Haskó, and P. Pacher. 2007. Simple quantitative detection of mitochondrial superoxide production in live cells. *Biochem. Biophys. Res. Commun.* 358: 203–208.
39. Vayssier-Taussat, M., S. E. Kreps, C. Adrie, J. Dall'Ava, D. Christiani, and B. S. Polla. 2002. Mitochondrial membrane potential: a novel biomarker of oxidative environmental stress. *Environ. Health Perspect.* 110: 301–305.
40. Hajnóczky, G., G. Csordás, S. Das, C. Garcia-Perez, M. Saotome, S. Sinha Roy, and M. Yi. 2006. Mitochondrial calcium signalling and cell death: approaches for assessing the role of mitochondrial Ca2+ uptake in apoptosis. *Cell Calcium* 40: 553–560.
41. Lee, H. C., and Y. H. Wei. 2005. Mitochondrial biogenesis and mitochondrial DNA maintenance of mammalian cells under oxidative stress. *Int. J. Biochem. Cell Biol.* 37: 822–834.
42. Lee, H. C., P. H. Yin, C. W. Chi, and Y. H. Wei. 2002. Increase in mitochondrial mass in human fibroblasts under oxidative stress and during replicative cell senescence. *J. Biomed. Sci.* 9: 517–526.
43. Lee, H. C., P. H. Yin, C. Y. Lu, C. W. Chi, and Y. H. Wei. 2000. Increase of mitochondria and mitochondrial DNA in response to oxidative stress in human cells. *Biochem. J.* 348: 425–432.
44. Petrovas, C., Y. M. Mueller, I. D. Dimitriou, S. R. Altork, A. Banerjee, P. Sklar, K. C. Mounzer, J. D. Altman, and P. D. Katsikis. 2007. Increased mitochondrial mass characterizes the survival defect of HIV-specific CD8(+) T cells. *Blood* 109: 2505–2513.
45. Moncada, S., and J. D. Erusalimsky. 2002. Does nitric oxide modulate mitochondrial energy generation and apoptosis? *Nat. Rev. Mol. Cell Biol.* 3: 214–220.
46. Cayota, A., F. Vuillier, J. Siciliano, and G. Dighiero. 1994. Defective protein tyrosine phosphorylation and altered levels of p59fyn and p56lck in CD4 T cells from HIV-1 infected patients. *Int. Immunol.* 6: 611–621.
47. House, R. V., P. T. Thomas, and H. N. Bhargava. 1994. Comparison of immune functional parameters following in vitro exposure to natural and synthetic amphetamines. *Immunopharmacol. Immunotoxicol.* 16: 1–21.
48. Tallóczy, Z., J. Martinez, D. Joset, Y. Ray, A. Gácser, S. Toussi, N. Mizushima, J. D. Nosanchuk, J. Nosanchuk, H. Goldstein, et al. 2008. Methamphetamine inhibits antigen processing, presentation, and phagocytosis. *PLoS Pathog.* 4: e28.
49. Lin, M. T., and M. F. Beal. 2006. Mitochondrial dysfunction and oxidative stress in neurodegenerative diseases. *Nature* 443: 787–795.
50. Bonomini, F., S. Tengattini, A. Fabiano, R. Bianchi, and R. Rezzani. 2008. Atherosclerosis and oxidative stress. *Histol. Histopathol.* 23: 381–390.
51. Nishikawa, T., D. Edelstein, X. L. Du, S. Yamagishi, T. Matsumura, Y. Kaneda, M. A. Yorek, D. Beebe, P. J. Oates, H. P. Hammes, et al. 2000. Normalizing mitochondrial superoxide production blocks three pathways of hyperglycaemic damage. *Nature* 404: 787–790.
52. Martin, J. A., A. J. Klingelhutz, F. Moussavi-Harami, and J. A. Buckwalter. 2004. Effects of oxidative damage and telomerase activity on human articular cartilage chondrocyte senescence. *J. Gerontol. A Biol. Sci. Med. Sci.* 59: 324–337.
53. Chin, M. H., W. J. Qian, H. Wang, V. A. Petyuk, J. S. Bloom, D. M. Sforza, G. Laćan, D. Liu, A. H. Khan, R. M. Cantor, et al. 2008. Mitochondrial dysfunction, oxidative stress, and apoptosis revealed by proteomic and transcriptomic analyses of the striata in two mouse models of Parkinson's disease. *J. Proteome Res.* 7: 666–677.
54. Tain, L. S., R. B. Chowdhury, R. N. Tao, H. Plun-Favreau, N. Moisoi, L. M. Martins, J. Downward, A. J. Whitworth, and N. Tapon. 2009. Drosophila HtrA2 is dispensable for apoptosis but acts downstream of PINK1 independently from Parkin. *Cell Death Differ.* 16: 1118–1125.
55. Feske, S. 2007. Calcium signalling in lymphocyte activation and disease. *Nat. Rev. Immunol.* 7: 690–702.
56. Wan, B., K. F. LaNoue, J. Y. Cheung, and R. C. Scaduto, Jr. 1989. Regulation of citric acid cycle by calcium. *J. Biol. Chem.* 264: 13430–13439.
57. White, C., C. Li, J. Yang, N. B. Petrenko, M. Madesh, C. B. Thompson, and J. K. Foskett. 2005. The endoplasmic reticulum gateway to apoptosis by Bcl-X (L) modulation of the InsP3R. *Nat. Cell Biol.* 7: 1021–1028.
58. Nicholls, D. G. 2002. Mitochondrial function and dysfunction in the cell: its relevance to aging and aging-related disease. *Int. J. Biochem. Cell Biol.* 34: 1372–1381.
59. Gelderman, K. A., M. Hultqvist, A. Pizzolla, M. Zhao, K. S. Nandakumar, R. Mattsson, and R. Holmdahl. 2007. Macrophages suppress T cell responses and arthritis development in mice by producing reactive oxygen species. *J. Clin. Invest.* 117: 3020–3028.

60. Pubill, D., C. Chipana, A. Camins, M. Pallàs, J. Camarasa, and E. Escubedo. 2005. Free radical production induced by methamphetamine in rat striatal synaptosomes. *Toxicol. Appl. Pharmacol.* 204: 57–68.
61. Duchen, M. R. 2000. Mitochondria and calcium: from cell signalling to cell death. *J. Physiol.* 529: 57–68.
62. Perl, A., Y. Qian, K. R. Chohan, C. R. Shirley, W. Amidon, S. Banerjee, F. A. Middleton, K. L. Conkrite, M. Barcza, N. Gonchoroff, et al. 2006. Transaldolase is essential for maintenance of the mitochondrial transmembrane potential and fertility of spermatozoa. *Proc. Natl. Acad. Sci. USA* 103: 14813–14818.
63. Davidson, C., A. J. Gow, T. H. Lee, and E. H. Ellinwood. 2001. Methamphetamine neurotoxicity: necrotic and apoptotic mechanisms and relevance to human abuse and treatment. *Brain Res. Brain Res. Rev.* 36: 1–22.
64. Wu, C. W., Y. H. Ping, J. C. Yen, C. Y. Chang, S. F. Wang, C. L. Yeh, C. W. Chi, and H. C. Lee. 2007. Enhanced oxidative stress and aberrant mitochondrial biogenesis in human neuroblastoma SH-SY5Y cells during methamphetamine induced apoptosis. *Toxicol. Appl. Pharmacol.* 220: 243–251.
65. Pariente, J. A., C. Camello, P. J. Camello, and G. M. Salido. 2001. Release of calcium from mitochondrial and nonmitochondrial intracellular stores in mouse pancreatic acinar cells by hydrogen peroxide. *J. Membr. Biol.* 179: 27–35.
66. Lambert, A. J., B. Wang, J. Yardley, J. Edwards, and B. J. Merry. 2004. The effect of aging and caloric restriction on mitochondrial protein density and oxygen consumption. *Exp. Gerontol.* 39: 289–295.
67. López-Lluch, G., N. Hunt, B. Jones, M. Zhu, H. Jamieson, S. Hilmer, M. V. Cascajo, J. Allard, D. K. Ingram, P. Navas, and R. de Cabo. 2006. Calorie restriction induces mitochondrial biogenesis and bioenergetic efficiency. *Proc. Natl. Acad. Sci. USA* 103: 1768–1773.
68. Praticò, D., C. M. Clark, V. M. Lee, J. Q. Trojanowski, J. Rokach, and G. A. FitzGerald. 2000. Increased 8,12-iso-iPF2alpha-VI in Alzheimer's disease: correlation of a noninvasive index of lipid peroxidation with disease severity. *Ann. Neurol.* 48: 809–812.
69. Lyras, L., R. H. Perry, E. K. Perry, P. G. Ince, A. Jenner, P. Jenner, and B. Halliwell. 1998. Oxidative damage to proteins, lipids, and DNA in cortical brain regions from patients with dementia with Lewy bodies. *J. Neurochem.* 71: 302–312.
70. Bagasra, O., F. H. Michaels, Y. M. Zheng, L. E. Bobroski, S. V. Spitsin, Z. F. Fu, R. Tawadros, and H. Koprowski. 1995. Activation of the inducible form of nitric oxide synthase in the brains of patients with multiple sclerosis. *Proc. Natl. Acad. Sci. USA* 92: 12041–12045.
71. Haorah, J., D. Heilman, C. Diekmann, N. Osna, T. M. Donohue, Jr., A. Ghorpade, and Y. Persidsky. 2004. Alcohol and HIV decrease proteasome and immunoproteasome function in macrophages: implications for impaired immune function during disease. *Cell. Immunol.* 229: 139–148.
72. Potula, R., J. Haorah, B. Knipe, J. Leibhart, J. Chrastil, D. Heilman, H. Dou, R. Reddy, A. Ghorpade, and Y. Persidsky. 2006. Alcohol abuse enhances neuroinflammation and impairs immune responses in an animal model of human immunodeficiency virus-1 encephalitis. *Am. J. Pathol.* 168: 1335–1344.
73. Jeng, W., A. W. Wong, R. Ting-A-Kee, and P. G. Wells. 2005. Methamphetamine-enhanced embryonic oxidative DNA damage and neurodevelopmental deficits. *Free Radic. Biol. Med.* 39: 317–326.
74. Prlic, M., M. A. Williams, and M. J. Bevan. 2007. Requirements for CD8 T-cell priming, memory generation and maintenance. *Curr. Opin. Immunol.* 19: 315–319.
75. Sklavos, M. M., H. M. Tse, and J. D. Piganelli. 2008. Redox modulation inhibits CD8 T cell effector function. *Free Radic. Biol. Med.* 45: 1477–1486.
76. Williams, M. S., and J. Kwon. 2004. T cell receptor stimulation, reactive oxygen species, and cell signaling. *Free Radic. Biol. Med.* 37: 1144–1151.
77. Brown, J. M., M. S. Quinton, and B. K. Yamamoto. 2005. Methamphetamine-induced inhibition of mitochondrial complex II: roles of glutamate and peroxynitrite. *J. Neurochem.* 95: 429–436.
78. Burrows, K. B., G. Gudelsky, and B. K. Yamamoto. 2000. Rapid and transient inhibition of mitochondrial function following methamphetamine or 3,4-methylenedioxymethamphetamine administration. *Eur. J. Pharmacol.* 398: 11–18.
79. Wallace, D. C., and W. Fan. 2009. The pathophysiology of mitochondrial disease as modeled in the mouse. *Genes Dev.* 23: 1714–1736.
80. Milagros Rocha, M., and V. M. Victor. 2007. Targeting antioxidants to mitochondria and cardiovascular diseases: the effects of mitoquinone. *Med. Sci. Monit.* 13: RA132–RA145.